

## Observed Substrate Topography-Mediated Lateral Patterning of Diblock Copolymer Films

M. J. Fasolka, D. J. Harris,\* and A. M. Mayes

*Department of Materials Science and Engineering, Massachusetts Institute of Technology, Cambridge, Massachusetts 02139*

M. Yoon and S. G. J. Mochrie

*Department of Physics, Massachusetts Institute of Technology, Cambridge, Massachusetts 02139*

(Received 6 May 1997)

We study the morphology of symmetric diblock copolymer films with thicknesses below the bulk equilibrium period supported by both flat and corrugated substrates. In this thickness regime, the film morphology is characterized by the formation of uniformly sized lateral domains. On flat substrates, these domains are randomly arranged. In contrast, on corrugated substrates, similar films exhibit domains which decorate the peaks of the substrate corrugations. Our observations suggest a novel and simple scheme for the lateral nanometer scale patterning of diblock copolymer films. [S0031-9007(97)04284-1]

PACS numbers: 68.55.-a, 61.41.+e, 81.05.Ys, 81.65.Cf

Several schemes for developing nanotechnologies hinge upon the ability to create designed fine distributions of discrete chemically homogeneous domains. Such patterned systems may themselves be devices, as with so-called “nanoreactors” [1] used recently to synthesize nanometer scale metallic particles, or act as templates onto which device structures are built, as with quantum-dot devices [2,3]. Given this paradigm for device production, the utility of diblock copolymers has been amply noted [1,5–8]. Diblock copolymers consist of chemically different polymer chains covalently bonded at one end. This block connectivity limits phase separation to the scale of the block dimensions [4], resulting in the spontaneous creation of domains of uniform size and spacing, each on the order of tens of nanometers. This *microphase separation* behavior makes such materials attractive to nanotechnologists.

In practice, the use of diblock copolymers in device production has shown limitations [5–8]. One encompassing limitation arises from the fact that the domain patterns available for exploitation are restricted to the types of morphology these systems display. While, at first glance, this limitation seems absolute, in this Letter we propose a novel and simple scheme, applicable to the creation of nanostructured thin copolymer films, which relaxes this restriction. Specifically, through the use of topographically patterned supporting substrates, lateral domain patterns are created in copolymer films that mirror the substrate topography. This transduction of topographic information to film nanostructure is mediated through the dependence of copolymer morphology on film thickness.

Thin film copolymer morphology differs from that of the bulk in part due to the increased importance of surface interactions. Consider, for example, symmetric diblock copolymers, characterized by blocks of equal volume, which typically exhibit a lamellar microstructure with an equilibrium period  $L_0$ . In these films, the surface energy difference between the blocks demands the expression of the lower energy component at the film surfaces.

As a consequence, lamellae form lying parallel to the film surfaces [9,10]. More complex pictures develop when considering films whose thickness ( $t$ ) does not conform to an integral multiple of the equilibrium period  $L_0$ . For films thicker than  $L_0$  and  $t \neq nL_0$ , “terrace” defects, of height  $L_0$ , form on the film surface(s) [11]. When the film thickness is below  $L_0$ , its morphology is frustrated by the competition of several forces, including strong surface interactions, slow kinetics, and the “bulk” driving force towards a morphology with the natural period  $L_0$  [12–19]. The development of *laterally* ordered domains can allow such systems to preserve a semblance of the bulk morphological period of the material [14,15]. Here we study the morphology of supported sublamellar films of a specific diblock copolymer system and compare the distribution of lateral microphase domains in films supported by flat substrates to those deposited onto corrugated substrates. This comparison serves to both illuminate the effect of substrate topography on morphology and illustrate how substrate topography can be used to control diblock film morphology.

The polymer system investigated is a polystyrene-poly(*n*-butyl methacrylate) (PS-PnBMA) diblock copolymer. Anionically synthesized, it has a molecular weight of 250 K, with  $M_w/M_n = 1.12$ . The molecules are 55% PnBMA by volume. A bulk lamellar microstructure was verified by transmission electron microscopy (TEM). In thin films supported by silicon oxide substrates, surface-parallel lamellae form with an equilibrium period  $L_0 \approx 66$  nm. The expression of the PnBMA block at both the substrate and free surfaces was shown previously by neutron reflectivity measurements [18], and is expected, given the lower surface energy of PnBMA as compared to PS and the known affinity of methacrylates to oxide surfaces.

Flat supporting substrates were polished Si(100) wafers. Corrugated substrates were fabricated utilizing the faceting transformation of slightly misoriented Si(113) surfaces as described in detail in Refs. [19,20]. We employed

corrugated substrates with a sawtooth-like profile. Substrates exhibiting corrugations with average peak-to-peak periods of 80, 170, and 210 nm and respective average amplitudes of 2, 4, and 3.5 nm were used, as characterized by atomic force microscopy (AFM). In each case, native silicon oxide layers cover the substrate surfaces.

Films were deposited directly onto the substrates via spin casting from toluene. Excess solvent was removed under vacuum for 24 h. Annealing under vacuum at 170 °C for four days induced microphase separation in the films. Approximate film thicknesses were deduced by AFM height measurements (some on samples with exposed substrate), ellipsometry, and film color observations via optical microscopy. In particular, it was determined that where lateral patterning is observed, the film is  $\sim 30$  nm thick ( $t < L_0/2$ ). Characterization of film morphology was completed with TEM and AFM. Films were prepared for TEM by first peeling them from their substrates. This was accomplished by coating the annealed films with an evaporated carbon layer ( $\sim 10$  nm) and then covering this composite with a 25% aqueous solution of polyacrylic acid (PAA). Upon evaporation of the water this overlayer contracts, pulling the film, intact, from the substrate [21]. The film-(PAA) complex was then placed (PAA side down) onto a pool of deionized water, dissolving the PAA layer and leaving a floating sample (with supporting carbon layer) which was recovered on TEM grids. Some of these samples were treated to an additional protective carbon layer, embedded in epoxy media, and ultramicrotomed for examination in cross section. Contrast between the diblock components was enhanced by staining the PS block via a 10 min exposure to  $\text{RuO}_4$  vapor. Low dose TEM was performed in bright field at 200 KV on a Jeol 200-CX. AFM was performed in "tapping mode" on a DI Dimension 3000. Sample films were examined on their substrates. Domain contrast is due to elasticity differences between the diblock components [22]. The AFM probe tip depresses softer PnBMA regions relative to PS areas. This was verified by examining sample regions, e.g., defects on terrace edges [11], that were certain to express localized PnBMA domains at the surface. In that examination, and the AFM micrographs that follow, PnBMA domains appear as depressions  $\sim 1$  nm deep.

The plan view TEM micrograph in Fig. 1 shows a section of PS-PnBMA diblock film removed from a flat substrate. In this image, the film thickness decreases from right to left as reflected in the schematic cross section below. On the extreme right, labeled (A), the film has a thickness  $\approx L_0$  (66 nm). Here the diblock has formed a full lamella parallel to the substrate surface, and hence no contrast is observed. Moving to the left, the film decreases in thickness through a transition region (B) to the area labeled (C) where the film is approximately  $L_0/2$  thick. The domains visible in (B) are commonly observed "terrace edge defects" [11]. In region (C), the film achieves a

"half-lamellar" morphology. Here the PnBMA block resides at the substrate, while the PS is expressed at the free surface. While in terms of surface energetics this morphology is not optimal, PS being the higher energy component, this structure offers the minimum interfacial area between the immiscible PS and PnBMA domains and the maximum number of configurations for each block. As the film thickness decreases below  $L_0/2$  into region (D), lateral structure appears. Here a random array of uniformly sized, roughly circular PnBMA domains develops. Examination of similar films ( $t \sim 30$  nm  $< L_0/2$ ) with AFM (E) shows a similar random arrangement of regular domains, indicating that these regions amount to local expressions of PnBMA at the surface. The domain size, as measured by AFM, was found to be  $\sim 35$  nm, which is consistent with the PnBMA block dimensions.

This lateral structure was further examined by TEM in cross section, as shown in Fig. 2. In this micrograph, the film ribbon has been tilted with respect to the viewing plane, making its top surface visible [the light band above layer (A)]. In the cross-sectional portion of this projection [layers (A–D)], surface-parallel layers and distinct lateral domains are visible. The top (A) and bottom (D) layers are protective evaporated carbon layers introduced during the sample preparation. The dark band (B) is the stained PS layer, which originally resided at the free surface. The light layer (C), which originally resided adjacent to the substrate, is the PnBMA layer. While generally this layer lies parallel to the film surface, it is punctuated by occasional perpendicular structures (emphasized by arrows) which perforate the PS layer above. These semicolumnar structures are the lateral domains seen in the plan view TEM and AFM micrographs described above. In terms of thermodynamics, the formation of these structures is justified as follows. At  $t < L_0/2$ , chains forming a half-lamellar structure will have less available configurations than when  $t = L_0/2$ . To increase the configurational entropy, the lamella might adopt a perpendicular orientation [14,15]. For the present case, however, a fully perpendicular orientation would result in a large energetic loss at the substrate, where the interaction of PnBMA with the oxide layer is strongly preferred. Therefore, the film adopts what is, in essence, a "compromise" morphology, whereby semicolumns of PnBMA perforate the PS layer to increase the overall configurational entropy of the system, while maintaining a layer of PnBMA at the substrate. This morphology has the added benefit of expressing some PnBMA at the film surface, lowering the total surface tension.

Turning to the film morphology on corrugated substrates, we point to Fig. 3. Here an AFM micrograph [3(A)] shows the microstructure of the free surface of a PS-PnBMA diblock film supported by a corrugated substrate with a peak-to-peak period of 210 nm. The film thickness is just under  $L_0/2$ . As observed on flat films, lateral PnBMA domains have formed. However, here these domains have decorated the peaks of the corrugated

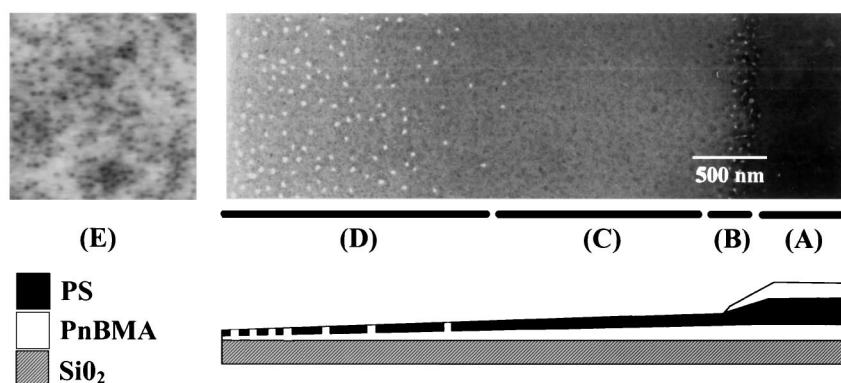


FIG. 1. Plan view TEM micrograph (right) showing film removed from a flat substrate which decreases in thickness moving from A to D. The diagram below shows the film in schematic cross section. The AFM micrograph (left, E) of a similar film is 1  $\mu\text{m}$  square.

substrate, forming a patterned film that reflects the topography beneath. Verification of the placement of PnBMA domains over the ridge peaks was determined through AFM images which included both the film pattern and bare substrate ridges.

Given the scheme for lateral domain formation described above, this pattern generation is easily understood. Figure 3(B) shows a schematic film cross section on a corrugated substrate. As illustrated, such lateral patterning occurs because the substrate topography creates a modulation of the film thickness. For as noted [21] the bottom film profile is corrugated, while AFM micrographs [Figs. 3(A) and 4(A)] indicate that the top surface is “flat,” showing no height variations correlating with the substrate ridges beneath—an observation predicted theoretically for diblock films of this thickness on corrugated substrates of similar period [13]. Above the peaks, the film must be thinner; over the troughs, the film is thicker. So if the film is in a certain thickness regime (near  $L_0/2$ ), a condition is created such that over the peaks,  $t$  is below  $L_0/2$ , while in the troughs  $t$  is about  $L_0/2$ . In terms of morphology, the condition for lateral domain formation ( $t < L_0/2$ ) is created above the peaks, while half lamellae (which form when  $t \approx L_0/2$ ) are preferred in the troughs

[Fig. 3(C)]. The result, shown schematically in Fig. 3(D) and observed in Fig. 3(A), is a pattern of lateral domains that mirrors substrate topography.

What makes this phenomenon notable is the wide control it offers over lateral film morphology. Since the formation of lateral domains can be induced by local film thickness, it is likely that any design of substrate topography, provided it has appropriate amplitude, will be transduced into an analogous film pattern. Appropriate amplitude means that the substrate features are of such height that film thickness modulations about  $L_0/2$  are generated, a condition met by the corrugated substrates used here. Figure 4 demonstrates the control over film

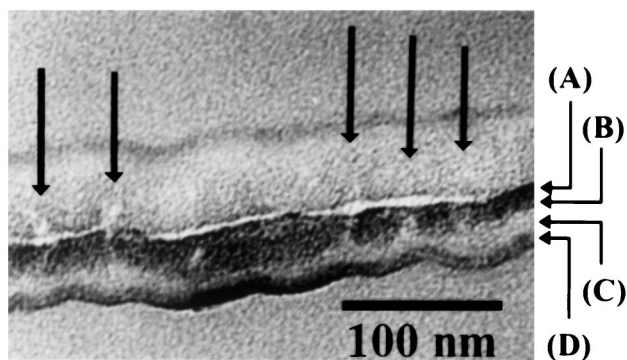


FIG. 2. Cross-sectional TEM of diblock film showing lateral domains (emphasized by vertical arrows).

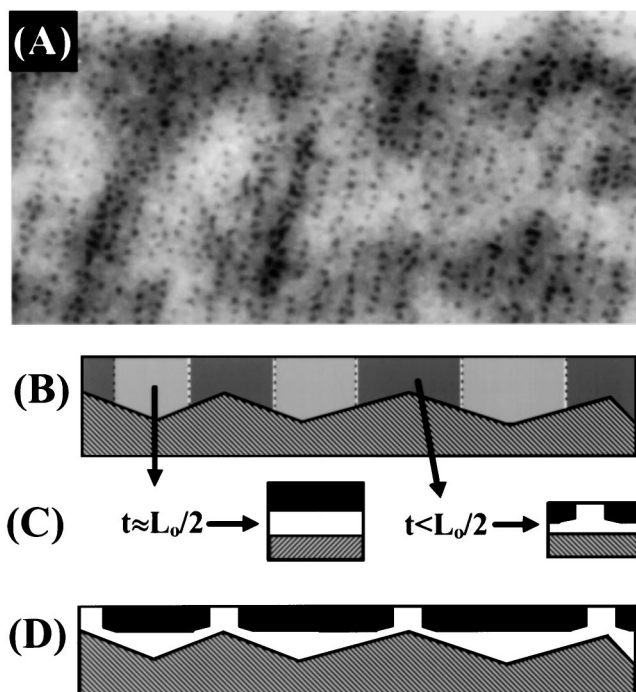


FIG. 3. AFM (A) of diblock film morphology on corrugated substrates. This image is  $5 \times 2.5 \mu\text{m}$ . The diagrams (B)–(D) below illustrate why the lateral patterning occurs.

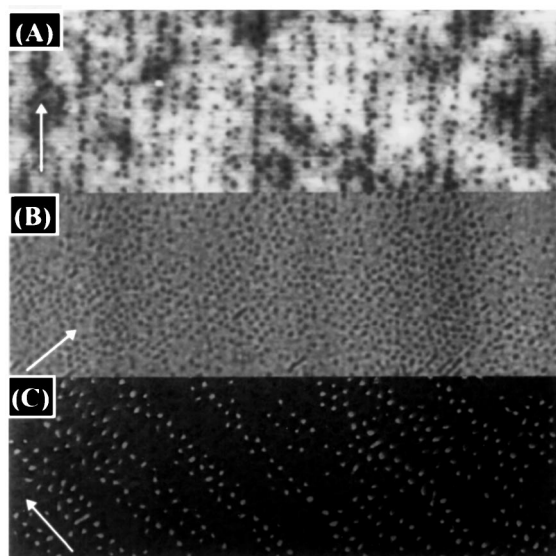


FIG. 4. (A),(B) AFM micrographs of films on corrugated substrates with 170 and 80 nm periods, respectively. These images are  $5 \mu\text{m}$  wide. (C) TEM of thinner film on a 210 nm period corrugated substrate. This image is  $3 \mu\text{m}$  wide. White arrows show the direction of ridge orientation.

patterning that can be exercised. Here AFM and TEM micrographs show how the film morphology can be modified by varying the corrugation period and the average film thickness. Figures 4(A) and 4(B) illuminate the effect of the corrugation period, where the 170 nm [Fig. 4(A)] and 80 nm [Fig. 4(B)] substrate periods are echoed in the film morphology. Comparing Figs. 4(A) and 4(C), we see the effect of changing the average film thickness. While the substrates in Figs. 4(A) and 4(C) have similar periods (170 and 210 nm, respectively) the average film thickness in Fig. 4(C) is smaller. Decreasing the average film thickness causes a wider band of material over the substrate peaks to meet the condition for forming lateral domains. Accordingly, multiple rows of domains are seen in Fig. 4(C), while only single rows are seen in Fig. 4(A). Additionally, these micrographs indicate that the closest spacing of lateral domains *along* the peak direction remains relatively constant ( $\sim 80$  nm by AFM), and appears to be characteristic of the material.

In conclusion, we have described the morphology of films of symmetric PS-PnBMA diblock copolymers in the sublamellar thickness regime. Here the film morphology is characterized by lateral PnBMA domains. When such films are supported by flat substrates, these uniformly sized domains are distributed randomly, while films on corrugated substrates exhibit domains which decorate the ridge peaks. This occurs because the film morphology is thickness dependent while the substrate topography produces a pattern of film thickness. As demonstrated, a range of film morphologies can be created by changing the substrate topography. Given such control, this phenomenon shows potential for use in nanoscale device fabrication.

We acknowledge B.L. Carvalho, L.H. Radzilowski, and E.L. Thomas for useful discussions. This work was partially supported by the MRSEC program of the National Science Foundation under Awards No. DMR-9400334 and No. DMR-9423641.

\*Current address: Polymer Science and Engineering Department, University of Massachusetts, Amherst, MA.

- [1] See, for example, J. P. Spatz, A. Roescher, and M. Moller, *Adv. Mater.* **8**, 337 (1996); B.H. Sohn and R.E. Cohen, *Acta Polymer* **47**, 340 (1996), and references therein.
- [2] See, for example, L. Brus, *Appl. Phys. A* **53**, 465 (1991), and references therein.
- [3] S. Y. Shiryayev, F. Jensen, J. Lundsgaard Hansen, J. Wulff Petersen, and A. Nylandsted Larson, *Phys. Rev. Lett.* **78**, 503 (1997).
- [4] See, for example, M. Shibayama, T. Hashimoto, and H. Kawai, *Macromolecules* **16**, 1434 (1983); E. Helfand and Z.R. Wasserman, in *Developments in Block Copolymers*, edited by I. Goodman (Applied Science, Essex, England, 1982), Vol. 1.
- [5] T.L. Morkved, M. Lu, A.M. Urbas, E.E. Ehrichs, H.M. Jaeger, P. Mansky, and T.P. Russell, *Science* **273**, 932 (1996).
- [6] P. Mansky, C.K. Harrison, P.M. Chaikin, R.A. Register, and N. Yao, *Appl. Phys. Lett.* **68**, 2586 (1996).
- [7] J.P. Spatz, S. Sheiko, and M. Moller, *Adv. Mater.* **8**, 513 (1996).
- [8] M. Park, C. Harrison, P.M. Chaikin, R.A. Register, and D.H. Adamson, *Science* **276**, 1407 (1997).
- [9] S.H. Anastasiadis, T.P. Russell, S.K. Satija, and C.F. Majkrzak, *Phys. Rev. Lett.* **62**, 1852 (1989).
- [10] G.H. Fredrickson, *Macromolecules* **20**, 2535 (1987).
- [11] B.L. Carvalho and E.L. Thomas, *Phys. Rev. Lett.* **73**, 3321 (1994).
- [12] T.P. Russell, A. Menelle, S.H. Anastasiadis, S.K. Satija, and C.F. Majkrzak, *Macromolecules* **24**, 6263 (1991).
- [13] M.S. Turner and J.-F. Joanny, *Macromolecules* **25**, 6681 (1992).
- [14] D.G. Walton, G.J. Kellogg, A.M. Mayes, P. Lambooy, and T.P. Russell, *Macromolecules* **27**, 6225 (1994).
- [15] G.J. Kellogg, D.G. Walton, A.M. Mayes, P. Lambooy, T.P. Russell, P.D. Gallager, and S.K. Satija, *Phys. Rev. Lett.* **76**, 2503 (1996).
- [16] T.L. Morkved and H.M. Jaeger, *Europhys. Lett.* (to be published).
- [17] L.H. Radzilowski, B.L. Carvalho, and E.L. Thomas, *J. Polym. Sci. B* **34**, 3081 (1996).
- [18] P. Mansky, T.P. Russell, and S.K. Satija (unpublished).
- [19] S. Song and S.G.J. Mochrie, *Phys. Rev. B* **51**, 10068 (1995).
- [20] S. Song, S.G.J. Mochrie, and G.B. Stephenson, *Phys. Rev. Lett.* **74**, 5240 (1995).
- [21] AFM was used to characterize the substrate side of the films after removal. They were found to replicate the substrate surface exactly, indicating that films remain intact through the preparation process.
- [22] B.K. Annis, D.W. Shwark, J.R. Reffner, E.L. Thomas, and B. Wunderlich, *Makromol. Chem.* **193**, 2589 (1992).